Interaction between Myoglobin and Hyaluronic Acid in Their Layer-by-Layer Assembly: Quartz Crystal Microbalance and Cyclic Voltammetry Studies

Hongyun Liu and Naifei Hu*

Department of Chemistry, Beijing Normal University, Beijing 100875, China

Received: February 28, 2006; In Final Form: April 17, 2006

Myoglobin (Mb), with different net surface charges at different pH in buffers and negatively charged hyaluronic acid (HA) at pH 5.0 in solutions were alternately adsorbed onto various solid surfaces and successfully assembled into $\{Mb/HA\}_n$ layer-by-layer films. The Mb in $\{Mb/HA\}_n$ films showed a quasi-reversible cyclic voltammetry (CV) response for its heme Fe^{III}/Fe^{II} redox couple. Quartz crystal microbalance (QCM) and CV were used to confirm the film growth and characterize the films. The interaction between Mb and HA and the influencing factors for Mb adsorption on HA surface, such as pH, Mb concentration, and ionic strength, were investigated in detail. The assembly driving force for $\{Mb/HA\}_n$ films, especially for the films assembled with like-charged Mb and HA, was found to be of electrostatic origin, while the secondary interaction such as hydrophobic interaction also plays an important role in some circumstances. Although the growth of $\{Mb(pH\ 7.0)/HA\}_n$ and $\{Mb(pH\ 9.0)/HA\}_n$ films was linear with the adsorption step, the exponential growth of $\{Mb(pH\ 5.0)/HA\}_n$ films was observed, especially when the films became thick. This exponential increase of mass and thickness with deposition step for $\{Mb(pH\ 5.0)/HA\}_n$ films was most probably attributed to the diffusion mechanism in which some HA molecules could diffuse in to and out of the whole films during the film assembly. Atomic force microscopy (AFM) results supported this speculation. UV−vis and IR spectroscopies of $\{Mb/HA\}_n$ films, combined with the comparative CV experiments of $\{Mb/HA\}_n$ and $\{catalase/HA\}_n$ films, suggest that Mb in the $\{Mb/HA\}_n$ multilayer films retains its near-native structure.

1. Introduction

Well-defined spatial organization of proteins or enzymes on solid surface without altering their original conformations and bioactivities is highly desired for development of biodevices such as biosensors and bioreactors, and exploration of methods for immobilization of proteins on the surface is still a great challenge in biorelated sciences.[1,2] In recent decades, a technique for construction of ultrathin films based on alternate adsorption of oppositely charged polyelectrolytes from their aqueous solutions has been developed and named "layer-by-layer assembly".[3−5] The polyelectrolyte multilayer films have a great application potential in a variety of fields and advantages of precise tailoring of film composition and thickness with simplicity and versatility. Currently, this technique has been extended to fabrication of protein films with a predesigned architecture on the nanometer scale.[6,7] The layer-by-layer films have demonstrated a significant potential in immobilization of proteins and application for constructing biodevices. For example, the layer-by-layer films of heme proteins or enzymes with polyelectrolytes assembled on the electrode surface display direct electrochemical responses for their heme Fe^{III}/Fe^{II} redox couples and electrocatalyze reduction of various substrates, which may establish a foundation for fabricating the new generation of electrochemical biosensors or bioreactors without using chemical mediators.[8−10]

The development of protein layer-by-layer assembly requires the first and profound understanding of the essence of interaction between proteins and polyions, driving forces of protein adsorption, and mechanism of film growth. The main driving force for layer-by-layer assembly is usually electrostatic interactions between oppositely charged substances.[3] However, when proteins are involved, the situation may become more complicated since the charge property and distribution on the protein surface are not homogeneous and uniform and may be variable with the surrounding environment such as pH. While most protein multilayer films are fabricated with oppositely charged proteins and polyelectrolytes, the "counterintuitive" phenomenon has also been reported where the layer-by-layer films with like-charged proteins and polyelectrolytes are successfully built up.[11−14] As for the growth mode, the layer-by-layer films of proteins and polyelectrolytes usually grow linearly with the number of bilayers (n), indicating the uniform increase of the films. However, the exponential growth of protein layer-by-layer films with adsorption step has been reported for $\{hyaluronic\ acid/collagen\}_n$ films,[15] where collagen is a kind of protein with a rope-like fiber shape. Exponential growth was also observed for some specific $\{polycation/polyanion\}_n$ layer-by-layer films under suitable conditions.[16−21] There are two possible explanations for this nonlinear growth of $\{polycation/polyanion\}_n$ films. On one hand, the surface roughness may increase with n, leading to the corresponding increase of the actual area of film surface and then resulting in more adsorption amounts of polyions in the next assembly step.[16,17] On the other hand, some polyions constituting the multilayer films may not only be adsorbed on the film surface, but also be "absorbed" into the films.[22,23] These absorbed "free" polyions inside the films may diffuse out of the films in the next adsorption step and combine with oppositely charged polyelectrolytes on the film surface, leading to the increase of adsorption amounts.

Hyaluronic acid or hyaluronan (HA) is a kind of linear polysaccharide consisting of linked disaccharide monomer units

* Corresponding author. Phone: +86 10 5880 5498. Fax: +86 10 5880 2075. E-mail: hunaifei@bnu.edu.cn.

10.1021/jp061271k CCC: $33.50
Published on Web 07/01/2006

SCHEME 1: Chemical Structures of (A) Hyaluronic Acid (HA) and (B) Chitosan (CS)

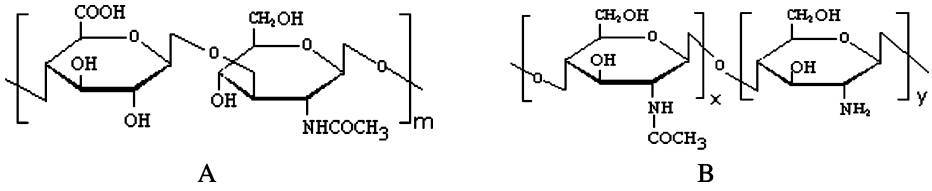

A B

of glucuronic acid and *N*-acetylglucosamine, and its chemical structure is shown in Scheme 1. As a weak polyelectrolyte with pK_a at 2.9,[24] HA demonstrates a relatively low charge density even when its all carboxylic acid groups are ionized since only one unit from the two in its monomer has an ionizable group. HA has been widely used in biomedicine because of its good biocompatibility and nontoxicity,[24] and its hydrogel membrane has also been applied in tissue engineering or drug delivery.[25] The unique structure and properties of HA make it become an often-used material with negative charges in layer-by-layer assembly. For example, some references have reported the layer-by-layer assembly of HA with chitosan (CS), another polysaccharide with positively charged groups on its backbone at suitable pH (Scheme 1).[23,26] The {CS/HA}$_n$ multilayer films showed an exponential growth of the film mass and thickness with the number of deposited layers.[23,26] Proteins, such as myoglobin (Mb), could be absorbed into the highly porous {CS/HA}$_n$ films.[27]

In the present work, myoglobin (Mb), a heme protein with a prosthetic heme group as its redox center, was used as the model protein. The layer-by-layer films of Mb with HA were successfully assembled on various substrates under different conditions. The interaction between Mb and HA and the influencing factors for Mb adsorption on HA surface were investigated systematically. The driving force for the film assembly, especially for that assembled by likely charged Mb and HA, was discussed in detail. When the pH of Mb adsorbate solution was set at 5.0, where Mb had net positive surface charges, the growth of {Mb/HA}$_n$ films was observed to be exponential with the number of adsorption steps, and a possible explanation for this was explored. To the best of our knowledge, exponential growth of layer-by-layer films of globular proteins and polyelectrolytes has not been reported until now. In addition, the conformation of Mb in {Mb/HA}$_n$ films was studied by UV−vis and IR spectroscopies and comparative CV experiments with {catalase/HA}$_n$ films.

2. Materials and Methods

2.1. Chemicals. Horse heart myoglobin (Mb, M_w 17 800), bovine liver catalase (Cat, EC 1.11.1.6, M_w 240 000), bovine hemoglobin (Hb, M_w 66 000), hyaluronic acid (HA, $M_w \approx$ 400 000), chitosan (CS, the degree of deacetylation is more than 85%), 3-mercapto-1-propanesulfonate (MPS, 90%), and poly(diallyldimethylammonium chloride) (PDDA, 20%, $M_w \approx$ 60 000) were purchased from Sigma-Aldrich and used as received.

Buffers were 0.05 M acetate (pH 5.0), sodium dihydrogen phosphate (pH 7.0), and boric acid (pH 9.0), the pH of which was adjusted with HCl or NaOH solutions. All buffers contained 0.1 M KBr as supporting electrolyte unless mentioned otherwise. All water used was purified twice successively by ion exchange and distillation.

2.2. Film Assembly. For electrochemical experiments, basal plane pyrolytic graphite (PG, Advanced Ceramics, geometric area 0.16 cm^2) disk electrodes were abraded on metallographic sandpapers while flushing with water and then ultrasonicated in water for 30 s and dried in air. The PG electrodes were alternately immersed into 1 mg mL^{-1} solutions of CS and HA at pH 5.0 containing 0.5 M NaCl for 20 min with intermediate water washing, forming a two-bilayer {CS/HA}$_2$ precursor film on the PG surface. The role of precursor films is to make the electrode surface smoother and favor the following {protein/HA}$_n$ film buildup. AFM experiments confirmed that the smoothness of the surface improved greatly after the deposition of {CS/HA}$_2$ precursor films, although the surface may not be fully covered by the films according to Picart and co-workers.[23] The {protein/HA}$_n$ layer-by-layer films were then fabricated on the PG/{CS/HA}$_2$ surface. HA has negative surface charges at pH 5.0 with its pK_a at 2.9.[24] With the isoelectric point (pI) at 6.8,[28] Mb has net positive surface charges at pH 5.0, has net negative charges at pH 9.0, and is essentially neutral at pH 7.0. The {Mb/HA}$_n$ layer-by-layer films assembled by negatively charged HA and Mb with different charge states at three different pHs are designated as {Mb(pH 5.0)/HA}$_n$, {Mb(pH 7.0)/HA}$_n$, and {Mb(pH 9.0)/HA}$_n$. Taking the assembly of {Mb(pH 5.0)/HA}$_n$ films as an example, the PG/{CS/HA}$_2$ electrodes were alternately immersed for 20 min in 1 mg mL^{-1} Mb solutions at pH 5.0 and 1 mg mL^{-1} HA solutions at pH 5.0 (containing 0.5 M NaCl) with intermediate water washing, forming PG/{CS/HA}$_2$/{Mb(pH 5.0)/HA}$_n$ layer-by-layer films with the desired number of bilayers (n). The assembly of {Cat/HA}$_n$ films was similar but with 3 mg mL^{-1} Cat adsorbate solution at pH 4.0.

For the quartz crystal microbalance (QCM) study, gold-coated QCM resonator electrodes (geometric area 0.196 cm^2, fundamental frequency 8 MHz) were soaked in piranha solution (3:7 volume ratio of 30% H_2O_2 and 98% H_2SO_4. *Caution: piranha solution should be handled with extreme care, and only small volumes should be prepared at any time*) for 10 min and then washed in pure water and ethanol successively. The gold electrodes were then immersed in 4 mM 3-mercapto-1-propanesulfonate (MPS) ethanol solutions for 24 h to chemsorb a MPS monolayer and introduce negative charges on the Au surface. The procedure to build up {CS/HA}$_2$/{protein/HA}$_n$ films on the Au/MPS surface was the same as that on PG electrodes. After each adsorption step, the gold resonator electrodes were washed in water, dried in N_2 stream for 2 min to remove the adsorbed water, and then measured by QCM at its fundamental frequency in air. The influence of water adsorbed on the film surface would thus be negligible in the QCM measurements, while some strongly bound water within the films may still exist. On the basis of the Sauerbrey equation,[29] $\Delta F = -2F_0^2A^{-1}(\mu\rho_0)^{-1/2}\Delta m$, where F_0 is resonant frequency of the fundamental mode of the quartz crystal (8 MHz), μ is the shear modulus of quartz (2.947×10^{11} g cm^{-1} s^{-2}), ρ_0 is the density of the crystal (2.648 g cm^{-3}), and A is the geometric area of the QCM electrode (0.196 cm^2), the frequency shift, ΔF (Hz), would be proportional to the adsorbed mass, Δm (g), by taking into account the properties of quartz resonator used in this work. Thus, 1 Hz of frequency decrease corresponds to 1.35 ng of mass increase. The nominal thickness, d (cm), can be expressed by $d = -3.4 \times 10^{-9}\ \Delta F/\rho$, where ρ

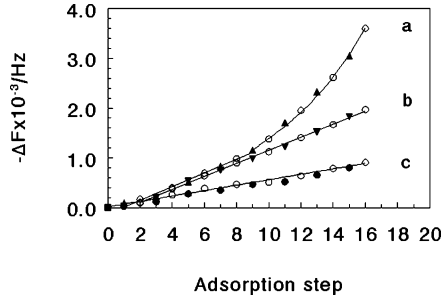

Figure 1. Shift of QCM frequency with adsorption step for (a) {Mb(pH 5.0)/HA}$_n$, (b) {Mb(pH 7.0)/HA}$_n$, and (c) {Mb(pH 9.0)/HA}$_n$ films with adsorption step for (■) MPS/{CS/HA}$_2$, (○) HA, (▲) Mb at pH 5.0, (▼) Mb at pH 7.0, and (●) Mb at pH 9.0.

is the density of the adsorbed layer material (g cm^{-3}). For the polymer HA, the density was around 1.2 ± 0.1 g cm^{-3},[30] while for the protein, the density was about 1.3 ± 0.1 g cm^{-3}.[31]

The {protein/HA}$_n$ films on Au QCM electrodes were also used for reflectance absorption infrared (RAIR) spectroscopy. For the UV−vis spectroscopic study, quartz slides (1 × 4 cm^2, 1-mm thick) were immersed in freshly prepared piranha solution for 20 min, rinsed with water, and dried with nitrogen stream. The {CS/HA}$_2$/{Mb/HA}$_n$ films were then assembled with the same procedure as that on PG electrodes. For atomic force microscopy (AFM) study, silicon wafers were treated by piranha solution and then washed in pure water and ethanol successively, making the surface of the wafers hydrophilic. A PDDA/HA precursor bilayer was built up on the surface, and the following procedure to fabricate {Mb/HA}$_n$ films was the same as that on PG/{CS/HA}$_2$ electrodes.

2.3. Apparatus and Procedures. A CHI 420 electrochemical workstation (CH Instruments) was used for cyclic voltammetry (CV) and QCM studies. For CV, a three-electrode cell was used with a saturated calomel electrode (SCE) as the reference electrode, a platinum wire as the counter electrode, and a PG disk with films as the working electrode. CVs at film electrodes were performed in buffers containing no proteins. Buffers were purged with highly purified nitrogen for at least 15 min prior to a series of experiments. A nitrogen environment was then kept in the cell during the whole experiment. A NEXUS 670 FT-IR spectrophotometer (Nicolet) with OMNI-sampler-HATR accessory was used for RAIR spectroscopy. A Cintra 10e UV−visible spectrophotometer (GBC) was used for UV−vis spectroscopy. AFM experiments were preformed with a HL-II scanning probe microscope (Zhongke Jidian, Beijing). All experiments were run at an ambient temperature of 20 ± 2 °C.

3. Results

3.1. Layer-by-Layer Assembly of {Mb/HA}$_n$ Films. The growth of {Mb/HA}$_n$ films on the surface of {CS/HA}$_2$ precursor films on Au/MPS and PG electrodes was monitored or confirmed by QCM and CV, respectively. QCM results showed that for all three {Mb/HA}$_n$ films built up at different pH for Mb adsorbate solutions, the QCM frequency decreased with increasing number of Mb/HA bilayers (Figure 1), indicating the successful film assembly not only for the oppositely charged HA and Mb but also for the similarly charged components. At the same adsorption step, the frequency decrease demonstrated a sequence of pH 5.0 > 7.0 > 9.0 for both Mb and HA, as expected, since the repulsion between like-charged HA and Mb at pH 9.0 weakened the attraction between them. For {Mb(pH 7.0)/HA}$_n$ and {Mb(pH 9.0)/HA}$_n$ films, a roughly linear frequency decrease with adsorption steps was observed (Figure 1), indicating that the adsorption amount of Mb or HA is nearly constant in each bilayer at these specific pHs. However, for {Mb(pH 5.0)/HA}$_n$ films, the linearity of the dependence of QCM frequency shift on adsorption step was observed only for the first five bilayers. When $n > 5$, the $-\Delta F$ value increased exponentially with adsorption step up to at least $n = 8$ (Figure 1a). Taking $n = 5$ as an intersection, the average $-\Delta F$ value and corresponding Δm and d values of {Mb(pH 5.0)/HA}$_n$ films for $n \leq 5$ and $n > 5$ are separately listed in Table 1. Since the increase of the films above $n = 5$ was exponential, the listed values of $-\Delta F$ and the corresponding Δm and d for each bilayer in this case is just a very rough estimation and used only for comparison in some specific case. The QCM results of {Mb(pH 7.0)/HA}$_n$ and {Mb(pH 9.0)/HA}$_n$ films are also listed in Table 1 for comparison. The nominal thickness (d) of Mb for {Mb(pH 7.0)/HA}$_n$ and {Mb(pH 5.0)/HA}$_n$ ($n \leq 5$) films was 2.8 and 3.2 nm, respectively, roughly consistent with the dimension of Mb (2.5 × 3.5 × 4.5 nm^3 [32]), suggesting formation of a monomolecular layer for Mb in adsorption. For {Mb(pH 9.0)/HA}$_n$ films, the nominal thickness of 1.4 nm for Mb indicates very loosely packed Mb molecules in each adsorption layer, while for {Mb(pH 5.0)/HA}$_n$ ($n > 5$) films, the d value was estimated to be 8.1 nm, about two times larger than the Mb dimension, suggesting great aggregation of Mb in each adsorption layer. It should be pointed out that because of the nonideal situation, such as participation of residual electrolytes and water in the films, and the uncertainties in the estimation of film density and electrode area, the calculated Δm and d values are just a rough estimation with a reliability of about ±10% according to the literature.[6] Nevertheless, the general trend demonstrated in Figure 1 and Table 1 should be correct.

The {Mb/HA}$_n$ films were also assembled layer-by-layer on the surface of PG/{CS/HA}$_2$ electrodes. After each assembly cycle, the electrodes were rinsed with water and placed into pH 7.0 buffers, and CVs were then performed. Taking {Mb(pH 5.0)/HA}$_n$ films as an example, a pair of quasi-reversible CV reduction−oxidation peaks was observed at about −0.34 V vs SCE (Supporting Information, Figure S1), characteristic of the Mb heme Fe^{III}/Fe^{II} redox couple.[33] The peaks increased with the number of Mb/HA adsorption bilayers (n) up to 8. When $n > 8$, the CV peak current was essentially constant and did not increase any more, indicating that Mb in bilayers of $n > 8$ is no longer electroactive. In contrast, the PG/{CS/HA}$_2$ films with no Mb adsorbed showed no CV response at all in the same potential window. The {Mb(pH 7.0)/HA}$_n$ and {Mb(pH 9.0)/HA}$_n$ films showed similar character with the CV peak potential centered at a similar position but growth of peak currents with n up to $n = 6$. Thus, in the following experiments, $n = 6$ was usually used for comparison of different {Mb/HA}$_n$ films. For {Mb/HA}$_6$ films, the CV peak currents demonstrated a sequence of pH 5.0 > 7.0 > 9.0 (Figure 2A), in agreement with the QCM results. The CVs of {Mb/HA}$_n$ films also provided information on charging current which reflected the capacitance of double-layer formed at the electrode/solution interface. Compared with the bare PG electrodes (not shown), the charging current of {Mb/HA}$_n$ films was much smaller. This was mainly because the rough PG surface became smoother after assembly of layer-by-layer films on the surface, inducing the decrease of actual surface area. Another possibility is a decrease of the dielectric constant after film formation, which would also result in a decrease of double-layer capacitance.[34]

For a specific {Mb/HA}$_n$ film at the fixed n, both CV reduction and oxidation peak currents increased linearly with scan rates in the range from 0.05 to 2.0 V s^{-1}, the reduction

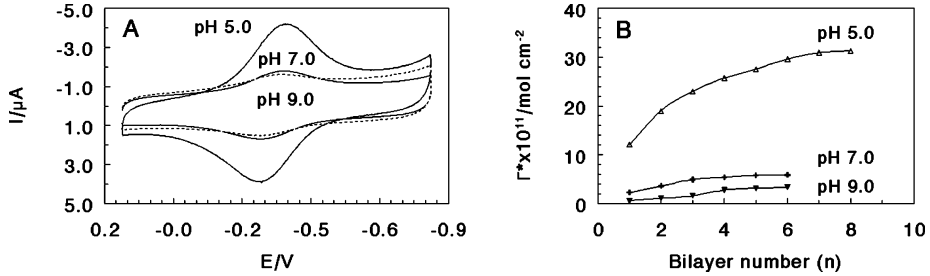

Figure 2. (A) CVs at 0.2 V s^{-1} in pH 7.0 buffers for $\{Mb/HA\}_6$ films assembled with Mb adsorbate solution at pH 5.0, 7.0, and 9.0. (B) Influence of the number of bilayers (n) on the surface concentration of electroactive Mb (Γ^*) estimated by integration of CV reduction peak at 0.2 V s^{-1} in pH 7.0 buffers.

TABLE 1: QCM Results in Each Bilayer for $\{Mb/HA\}_n$ Films on Au/MPS/$\{CS/HA\}_2$ Surface

	Mb			HA		
films	$-\Delta F$/Hz	Δm/ng	d/nm	$-\Delta F$/Hz	Δm/ng	d/nm
$\{Mb(pH\ 5.0)/HA\}_n$ ($n \le 5$)	122 ± 38	165	3.2	161 ± 18	217	4.6
$\{Mb(pH\ 5.0)/HA\}_n$ ($n > 5$)	308 ± 55	416	8.1	329 ± 151	444	9.4
$\{Mb(pH\ 7.0)/HA\}_n$	106 ± 37	143	2.8	140 ± 42	189	4.0
$\{Mb(pH\ 9.0)/HA\}_n$	52 ± 36	70	1.4	98 ± 42	132	2.8

TABLE 2: Electrochemical Parameters for $\{Mb/HA\}_6$ Layer-by-Layer Films Assembled at Different pH on PG/$\{CS/HA\}_2$ Surface[a]

pH	$E°$/V	E_{pc}/V	E_{pa}/V	ΔE_p/mV	Γ^*/(mol cm^{-2})
5.0	−0.343	−0.379	−0.307	72	2.0×10^{-10}
7.0	−0.340	−0.373	−0.306	67	5.4×10^{-11}
9.0	−0.349	−0.383	−0.315	68	3.6×10^{-11}

[a] Data from CVs at 0.2 V s^{-1} in pH 7.0 buffers.

and oxidation peaks showed symmetric shape and almost equal height, and integration of the CV reduction peak at different scan rates gave nearly constant charge (Q) values, all indicating the diffusionless and thin-layer voltammetric behavior of Mb in the films.[35] In this case, integration of the CV reduction peak would give the total charge passing through the electrode in full reduction of Mb in the films and could be converted to the surface concentration of electroactive Mb (Γ^*, mol cm^{-2}).[35] All three $\{Mb/HA\}_n$ films displayed a nonlinear increase of Γ^* with n until 6 or 8, and afterward the Γ^* value reached the steady state (Figure 2B). With the same n, Γ^* showed a sequence of $\{Mb(pH\ 5.0)/HA\}_n > \{Mb(pH\ 7.0)/HA\}_n > \{Mb(pH\ 9.0)/HA\}_n$, also consistent with the results of QCM. The electrochemical parameters estimated by CV for $\{Mb/HA\}_6$ films assembled at different pH are listed in Table 2 for comparison. In the estimation of ΔE_p, while the influence of ohmic drop could not be ruled out completely, it would be very limited since the uncompensated resistance of the film electrodes was usually smaller than 100 Ω. Three types of $\{Mb/HA\}_6$ films on PG electrodes showed excellent stability. The peak potentials and currents were essentially unchanged for at least 1 month when the film electrodes were stored in pH 7.0 buffers.

3.2. Exponential Growth of Layer-by-Layer Films. Both HA and CS are classified as weak polyelectrolytes. HA has its pK_a value at 2.9,[24] and the pK_a of CS is at about 6.[36] Thus, at pH 5.0, HA is negatively charged and CS is positively charged, and $\{CS/HA\}_n$ films could be built up layer-by-layer on solid substrates mainly through electrostatic attraction between them. The typical profile for $\{CS/HA\}_n$ assembly measured by QCM showed an exponential dependence of the frequency shift on adsorption step (Figure 3A), similar to what was described by Richert et al.[23]

Exponential growth was also observed for $\{Mb(pH\ 5.0)/HA\}_n$ films, especially when the adsorption bilayer number became larger (Figure 1a). The same phenomenon was noticed when using different Mb concentrations and different ionic strengths in Mb dipping solution (Figure 3B). For example, when 0.5 mg mL^{-1} instead of 1 mg mL^{-1} Mb was used but keeping NaCl concentration at 0.1 M in adsorbate solution, the frequency change of $\{Mb(pH\ 5.0)/HA\}_n$ films became smaller at the same adsorption step but the film growth was still nonlinear (Figure 3B, curve a). If keeping the Mb concentration at 1 mg mL^{-1} but with higher NaCl concentration at 0.3 M, exponential growth of the films was also observed (Figure 3B, curve b). In addition, when hemoglobin (Hb), a heme protein with very similar properties to Mb but larger dimension, was assembled with HA into $\{Hb(pH\ 5.0)/HA\}_n$ layer-by-layer films, the exponential increase of frequency shift with adsorption step monitored by QCM was seen (Figure 3B, curve c). All these results indicate the generality of this nonlinear growth behavior for $\{protein/HA\}_n$ layer-by-layer films under suitable conditions.

3.3. AFM Study of $\{Mb(pH\ 5.0)/HA\}_n$ Films. The morphology of PDDA/HA/$\{Mb(pH\ 5.0)/HA\}_n$ films fabricated on the surface of silicon wafers was characterized by AFM either with Mb or HA as the outermost layer. When HA was the outermost layer, the surface became smoother with increasing number of adsorption bilayers (Figure 4a−d), while when Mb was the outermost layer, light spots or small "particles", which might represent the aggregation of Mb molecules, were observed (Figure 4e−h). With the same number of bilayers, the surface roughness for the films with Mb as the outermost layer was higher than that for the films with HA as the outermost layer. This difference was more pronounced after 10 bilayers were deposited as observed from Figure 4d and h. The interesting thing was that, with different number of bilayers, the Mb "particles" were not equally distributed on the surface when Mb was the outermost layer. The number of Mb "particles" on the film surface became more pronounced for the thicker $\{Mb(pH\ 5.0)/HA\}_n$ films, which was qualitatively consistent with exponential growth of the films observed by QCM.

3.4. Factors Affecting Mb Adsorption on the HA Layer. To further investigate the interaction between HA and Mb, the factors influencing Mb adsorption on HA layer surface, such as pH, concentration of Mb, and ionic strength in Mb adsorbate solution, were explored. CV and QCM were used to characterize the adsorption behavior of Mb on the PG/$\{CS/HA\}_2$ and Au/MPS/$\{CS/HA\}_2$ surface, respectively, under different conditions.

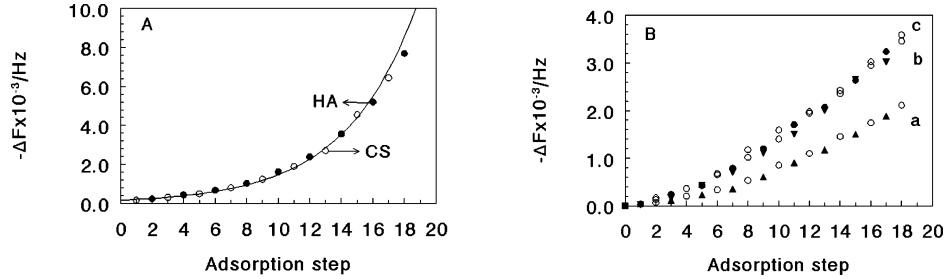

Figure 3. QCM frequency shift with adsorption step for (A) $\{CS/HA\}_n$ films on Au/MPS surface and (B) (a) $\{Mb(pH\ 5.0)/HA\}_n$ films with 0.5 mg mL^{-1} Mb containing 0.1 M NaCl, (b) $\{Mb(pH\ 5.0)/HA\}_n$ films with 1 mg mL^{-1} Mb containing 0.3 M NaCl, and (c) $\{Hb(pH\ 5.0)/HA\}_n$ films with 1 mg mL^{-1} Hb containing 0.1 M NaCl: (■) MPS/$\{CS/HA\}_2$, (○) HA, (▲) 0.5 mg mL^{-1} Mb (0.1 M NaCl), (▼) 1 mg mL^{-1} Mb (0.3 M NaCl), and (●) 1 mg mL^{-1} Hb (0.1 M NaCl) adsorption step. The line in A is a fitting line to the data with an exponential equation.

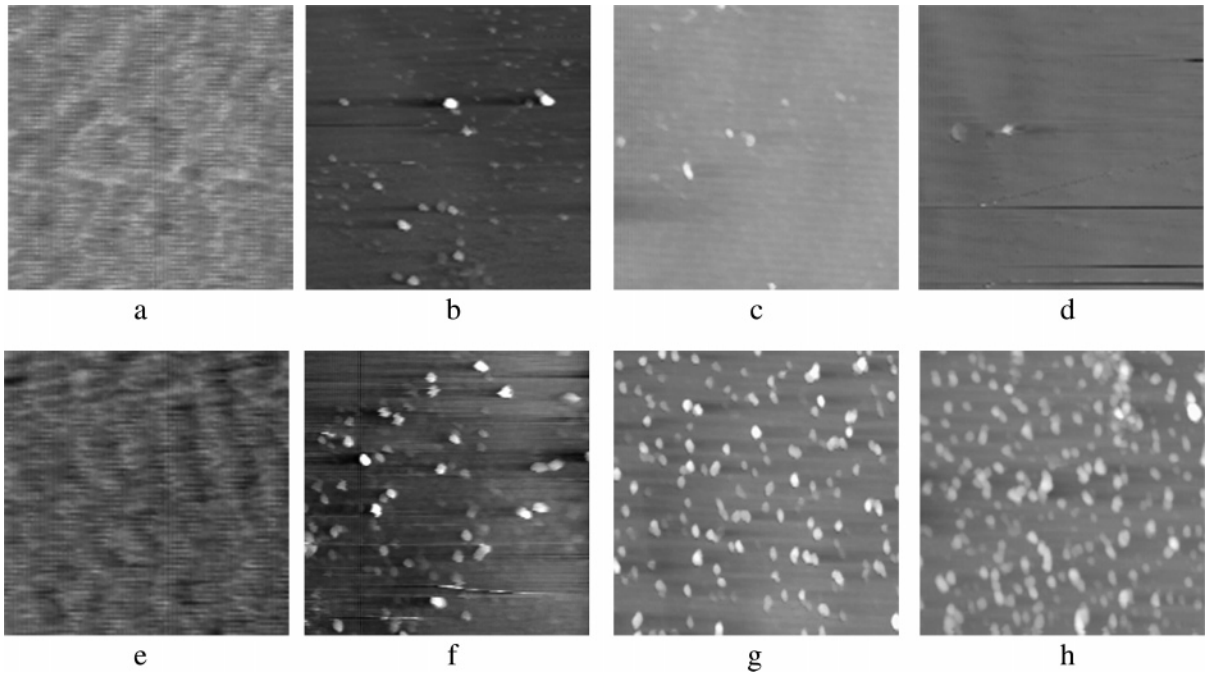

Figure 4. Top views of AFM images for (a) PDDA/HA, (b) PDDA/HA/$\{Mb/HA\}_6$, (c) PDDA/HA/$\{Mb/HA\}_8$, (d) PDDA/HA/$\{Mb/HA\}_{10}$, (e) PDDA/HA/Mb, (f) PDDA/HA/$\{Mb/HA\}_5$/Mb, (g) PDDA/HA/$\{Mb/HA\}_7$/Mb, and (h) PDDA/HA/$\{Mb/HA\}_9$/Mb films assembled on silicon wafers. The Mb adsorbate solution was at pH 5.0. The *X*-axis scale of the pictures is 1 μm.

With the same concentration of NaCl at 0.1 M, the dependence of Mb adsorption amount on Mb concentration (C_{Mb}) was explored at different pH. The PG/$\{CS/HA\}_2$ film electrodes were first immersed in Mb solutions for 20 min, then washed by water, and placed in blank buffers at pH 7.0. CVs were conducted in the buffers, and the surface concentration of electroactive Mb (Γ*) was measured by integration of the CV reduction peak. Under different pH conditions, Γ* increased with the Mb concentration up to about 1 mg mL^{-1} and then tended to level off (Figure 5). Thus, in most of our studies, 1 mg mL^{-1} was used as the optimal Mb concentration for the Mb dipping solution. With the same C_{Mb} value, Γ* showed a sequence of pH 5.0 > 7.0 > 9.0 in most cases except for the curves at pH 7.0 and pH 9.0 with very low Mb concentration.

The amount of adsorbed Mb on the $\{CS/HA\}_2$ surface was significantly affected by the ionic strength or the concentration of NaCl (C_{NaCl}) in Mb dipping solution (Figure 6). At different assembly pH, the profile of Γ^*-C_{NaCl} curves measured by CV showed a different trend (Figure 6A). At pH 5.0, with the increase of ionic strength, Γ* first increased at low NaCl concentration, reached a maximum at 0.3 M NaCl, and then decreased at higher C_{NaCl}. This trend was reversed when the pH of Mb adsorbate solution was at 9.0, in which Γ* values decreased with increasing ionic strength at low NaCl concentration and then increased with the ionic strength at high C_{NaCl}, passing through a minimum point at 0.3 M NaCl. At pH 7.0, Γ* values decreased with increasing C_{NaCl} at first; after reaching 0.3 M NaCl, the change tended to level off. In addition, the Γ* value of Mb at pH 7.0 became smaller than that at pH 9.0 when C_{NaCl} was larger than 0.1 M, showing the sequence pH 5.0 > 9.0 > 7.0. The influence of ionic strength in Mb adsorbate solution on the surface concentration of Mb (Γ, mol cm^{-2}) was also investigated by QCM, which displayed a similar trend to

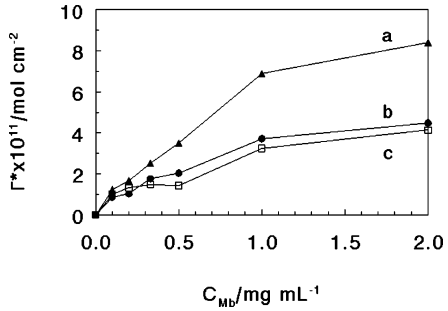

Figure 5. Influence of Mb concentration (C_{Mb}) on surface concentration of electroactive Mb (Γ*) estimated by CV at 0.2 V s^{-1} in pH 7.0 buffers on surface of $\{CS/HA\}_2$ films. Mb adsorbate solution contained 0.1 M NaCl at pH (a) 5.0, (b) 7.0, and (c) 9.0.

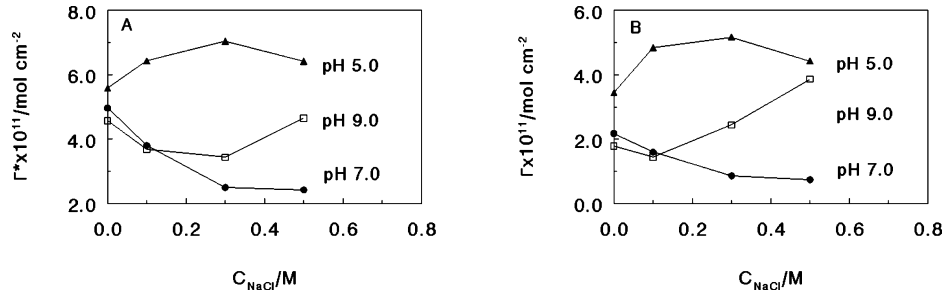

Figure 6. Effect of NaCl concentration in Mb adsorbate solution on (A) surface concentration of electroactive Mb (Γ*) measured by CV at 0.2 V s^{-1} in pH 7.0 buffers, and (B) surface concentration of Mb (Γ) estimated by QCM at different adsorbate pH on surface of $\{CS/HA\}_2$ films.

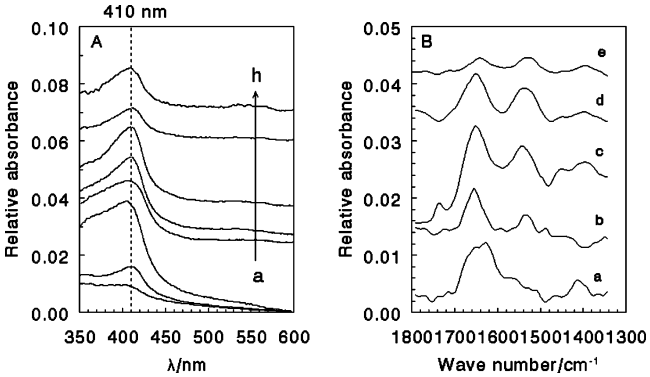

Figure 7. (A) UV−vis spectra of (a) dry $\{Mb(pH\ 9.0)/HA\}_8$, (b) dry $\{Mb(pH\ 7.0)/HA\}_8$, and (c) dry $\{Mb(pH\ 5.0)/HA\}_8$ films; $\{Mb(pH\ 5.0)/HA\}_8$ films in (d) pH 5.0, (e) pH 7.0, and (f) pH 9.0 buffers; (g) $\{Mb(pH\ 7.0)/HA\}_8$ and (h) $\{Mb(pH\ 9.0)/HA\}_8$ films in pH 7.0 buffers. (B) RAIR spectra of (a) HA, (b) Mb, (c) $\{Mb(pH\ 5.0)/HA\}_7$/Mb, (d) $\{Mb(pH\ 7.0)/HA\}_7$/Mb, and (e) $\{Mb(pH\ 9.0)/HA\}_7$/Mb films.

the CV results (Figure 6B). Generally, under the same conditions, the surface concentration of Mb measured by QCM (Γ) was a little smaller than that estimated by CV (Γ*). This difference is probably caused by the different roughness of PG and QCM Au electrodes. In estimating the surface concentration of Mb, the geometric area of electrodes was used without considering their roughness. However, since the roughness of PG was much larger than that of Au, the actual surface area of PG would be greater than that of Au. The difference in roughness between the two electrodes might become smaller after the adsorption of $\{CS/HA\}_2$ precursor films on electrode surface but still existed. These results also demonstrate that the Mb molecules adsorbed on PG/$\{CS/HA\}_2$ surface are nearly 100% electroactive and Γ* can be used to represent the adsorption amount of Mb in our study.

3.5. Conformation Studies. The shape and position of the Soret absorption band of the heme prosthetic group in heme proteins may provide information on protein conformation.[37,38] While the wavelength of the Soret band may not be a diagnostic criterion for the conformational variation of the whole protein, it is relatively sensitive to the conformational change in the heme region. UV−vis spectroscopy was thus performed to study the possible denaturation of Mb in $\{Mb/HA\}_8$ films assembled at different pH on quartz slides. For example, dry $\{Mb(pH\ 7.0)/HA\}_8$ and $\{Mb(pH\ 9.0)/HA\}_8$ films showed the Soret band at 410 nm, the same as that of dry Mb films. Dry $\{Mb(pH\ 5.0)/HA\}_8$ films demonstrated the Soret band at 408 nm, very close to that of dry Mb films alone (Figure 7A). This indicates that the microenvironment that the $\{Mb/HA\}_n$ films provide for Mb has no substantial influence on the conformation of incorporated Mb. The Soret band of three $\{Mb/HA\}_8$ films displayed a sequence in peak height of pH 5.0 > 7.0 > 9.0, consistent with the CV and QCM results. When $\{Mb(pH\ 5.0)/HA\}_8$ films were placed into buffer solutions at pH 5.0, 7.0, and 9.0, the position of the Soret band remained at 410 nm and the peak kept the well-defined shape (Figure 7A), suggesting that Mb in the films essentially retains its near-native structure in the medium pH range. In addition, after 1 month of storage of the $\{Mb(pH\ 5.0)/HA\}_8$ films in pH 7.0 buffers, the position of the Soret band and the peak shape showed little change, indicating that Mb in the films keeps its conformation for a quite long period. The same results were also observed for $\{Mb(pH\ 7.0)/HA\}_8$ and $\{Mb(pH\ 9.0)/HA\}_8$ films.

RAIR spectroscopy was also used to detect conformational change of Mb in $\{Mb/HA\}_n$ films. Figure 7B shows the typical RAIR spectra of pure HA and Mb films on Au substrates and $\{Mb/HA\}_7$/Mb films at different assembly pH on Au/MPS/$\{CS/HA\}_2$ surface. Pure Mb films showed IR amide I band at 1654 cm^{-1}, which was caused by C═O stretching vibration, and amide II band at 1541 cm^{-1}, which was attributed to the combination of N−H in-plane bending and C−N stretching vibration.[39,40] The pure HA films showed a broad IR peak in the amine I band region, which would interfere detection of the amide I band of Mb in $\{Mb/HA\}_n$ films, but did not show any IR absorption peak in the amine II band region. Thus, the amide II band of Mb in $\{Mb/HA\}_7$/Mb films would not be influenced by HA and was used to study the conformational change of Mb in the films. For all three $\{Mb/HA\}_7$/Mb films assembled under different pH conditions, the well-defined amide II peak was observed at 1540 cm^{-1}, which was very close to that of the amide II band for pure Mb films. While the IR spectra at this resolution may not be good enough to provide complete information about the folded state of the protein, the present data support the viewpoint that the major portion of Mb essentially retains its native structure in the $\{Mb/HA\}_n$ films.

To further confirm that Mb in $\{Mb/HA\}_n$ films retains its original structure and the heme prosthetic group of Mb does not come out of the Mb polypeptide matrix in the film environment, catalase (Cat) layer-by-layer films with HA were assembled with the same method and CV of the resulting $\{Cat/HA\}_n$ films was compared with that of $\{Mb/HA\}_n$ films. Cat is a heme enzyme with $M_w \approx 40\,000$ and is composed of four subunits, each of which contains one heme prosthetic group. With pI at about 5.8,[41] Cat has net positive surface charges at pH 4.0 and could be successfully assembled with negatively charged HA at pH 5.0 into $\{Cat/HA\}_n$ layer-by-layer films, which was confirmed by both QCM and CV (Supporting Information, Figures S2 and S3). A pair of quasi-reversible CV peaks was observed for $\{Cat/HA\}_n$ films at about −0.47 V vs SCE (Supporting Information, Figure S3A), characteristic of the Cat heme Fe^{III}/Fe^{II} redox couples.[42,43] While this peak pair was not very stable and gradually decreased with the number of bilayers (n), the peak potentials of $\{Cat/HA\}_n$ films were distinctly different from that of $\{Mb/HA\}_n$ films (Figure 8). $\{Cat/HA\}_n$ films exhibited the formal potential at −0.47 V,

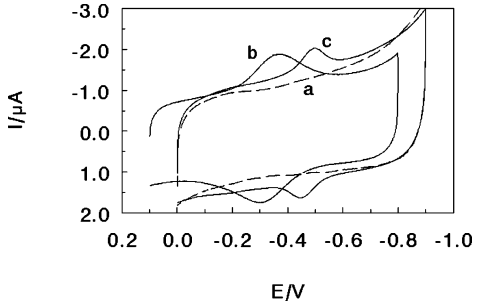

Figure 8. CVs at 0.2 V s^{-1} in pH 7.0 buffers for (a) $\{CS/HA\}_2$, (b) $\{CS/HA\}_2$/Mb, and (c) $\{CS/HA\}_2$/Cat films on PG electrodes.

about 130 mV more negative than that of the corresponding Mb films. If Mb and Cat in the films were denatured and most of the heme groups in the proteins were split out of the polypeptide matrix, the CV should have shown the peaks for free heme at the same position. The RAIR spectroscopic results of $\{Cat/HA\}_n$ films also indicate that Cat in $\{Cat/HA\}_n$ films essentially keep their native structure (Supporting Information, Figure S4). The results of both UV−vis and IR spectroscopic experiments (Figure 7), combined with the additional CV and IR results for $\{Cat/HA\}_n$ films, support the conclusion that Mb essentially retains its original structure without denaturation in $\{Mb/HA\}_n$ films.

4. Discussion

4.1. Driving Forces of Assembly. The QCM and CV results showed that not only Mb at pH 5.0 with net positive surface charges could be assembled into layer-by-layer films with negatively charged HA, but Mb at pH 9.0 with net negative surface charges or Mb at pH 7.0 with nearly "zero" net surface charges could also be successfully built up into multilayer films with HA (Figures 1 and 2, Table 1). These phenomena are difficult to explain with simple electrostatic interaction between Mb and HA, and the driving forces must involve a more complicated situation or character.

Adsorption of proteins on the surface of likely charged polyelectrolytes has also been reported in the literature previously,[11−14] and different explanations have been given. In the $\{Mb(pH\ 9.0)/HA\}_n$ system with both Mb and HA having net negative surface charges, two explanations are more reasonable. The first one is the charge reversal of Mb when the protein was adsorbed on the HA surface. The surface of the HA layer with negative charges tends to attract more protons from buffers, making the surface pH become lower than that in bulk solutions. Under suitable conditions, this lowering of pH on the HA surface may lead to the reversal of net surface charge of zwitterionic Mb from negative to positive. That is, the pH on the HA layer surface may change from higher than pI of Mb to lower than its pI, resulting in the adsorption of Mb on the HA surface. Biesheuvel and co-workers confirmed this possibility by theoretical modeling with similar systems.[44,45] Another explanation is the localized interaction between positively charged groups of Mb and HA. Mb has 19 lysine (Lys) and 2 arginine (Arg) residues on its surface, and their pK_a values are in the range of 10−12 and 12−13, respectively.[46,47] Thus, at pH 9.0, while Mb has net negative surface charges, there are still a lot of positively charged Lys and Arg groups on the Mb surface. Some of these positive residues may interact with oppositely charged HA by Coulombic attraction, leading to the adsorption of Mb on HA layer surface. The asymmetry and heterogeneity of protein charge distribution may make the binding sites on proteins with polyelectrolytes become localized, which has also been reported on other protein adsorption systems.[12−14]

While the two explanations are different, they involve electrostatic interaction in nature. This is further confirmed by the experiments of the ionic strength effect (Figure 6), since nonelectrostatic interactions such as hydrophobic interaction would not be influenced by ionic strength. For Mb at pH 5.0, when the concentration of NaCl (C_{NaCl}) in Mb adsorbate solution was below 0.3 M, the adsorption amount of Mb measured by CV (Γ^*) and QCM (Γ) increased with C_{NaCl}, while at C_{NaCl} higher than 0.3 M, the Γ^* or Γ value decreased with the ionic strength, having a maximum at 0.3 M NaCl (Figure 6). There are two contrary or opposite forces in Mb adsorption on the HA surface: the attraction between positively charged Mb and polyanionic HA and repulsion between two individual Mb molecules with the same positive charges. Both interactions are of electrostatic origin and are thus affected by the ionic strength. In the low ionic strength range, the repulsive interaction between Mb molecules may be the predominant force in Mb adsorption. The increase of C_{NaCl} would weaken the repulsive interaction between Mb molecules, leading to an increase of the amount of adsorbed Mb. On the contrary, in the high ionic strength range, the attractive interaction may become the dominant force. The increase of C_{NaCl} would reduce the interaction between Mb and oppositely charged HA because of the screening effect, resulting in a decrease of the amount of adsorbed Mb. It is therefore understandable that a peak-like curve in both Γ^*-C_{NaCl} and $\Gamma-C_{NaCl}$ plots was observed for Mb adsorption at pH 5.0, which usually comes out when two antagonist forces govern a physical process. A similar explanation could also be used to describe the appearance of a minimum value in Γ^*-C_{NaCl} and $\Gamma-C_{NaCl}$ curves at pH 9.0 for Mb adsorbate solution. The different trend of ionic strength on Mb adsorption amount between pH 5.0 and 9.0 may come from the different characters of interaction as described above.

At pH 7.0, Mb is actually neutral with no net surface charge. However, the localized electrostatic interaction between positive groups of Mb and HA may still exist. This Coulombic attraction can be weakened by the increase of ionic strength, causing a decrease of Γ^* or Γ in the low NaCl concentration range. However, when C_{NaCl} was larger than 0.3 M, Γ^* or Γ tended to level off and did not change with ionic strength, indicating that some nonelectrostatic interaction may become predominant. This speculation is further confirmed by the fact that the adsorption amount of Mb at pH 7.0 was not only less than that at pH 5.0, as expected, but also smaller than that at pH 9.0 when $C_{NaCl} >$ 0.1 M (Figure 6). This result may be explained by hydrophobic interaction between Mb and HA. When the pH in Mb adsorbate solution is 7.0 and the ionic strength is high enough, Mb may demonstrate strong hydrophobic character as for other proteins[48−51] while HA has also some hydrophobic property because of its low charge density and long polysaccharide bone. The hydrophobic interaction between Mb and HA may thus become the predominant force for adsorption of Mb on the HA surface in this case. As suggested in the literature,[52] hydrophobic attraction can play an important role for layer-by-layer buildup under certain circumstances. Generally, hydrophobic interaction is much weaker than electrostatic interaction, only about 1/800 of the latter in a vacuum and 1/13 in water,[53] and HA with negative charge also shows some hydrophilic character. All these may result in less adsorption of Mb at pH 7.0 than at pH 9.0 at high ionic strength. Thus, the profile of Γ^*-C_{NaCl} and $\Gamma-C_{NaCl}$ curves at pH 7.0 reflects the joint effect of both electrostatic and hydrophobic/hydrophilic interactions between Mb and HA.

4.2. Mechanism of Nonlinear Adsorption. The growth of layer-by-layer films of proteins with polyelectrolytes or nanoparticles with the number of bilayers (n) is usually linear. However, the growth of $\{Mb(pH\ 5.0)/HA\}_n$ films with n was nonlinear and exponential when n was large enough (Figure 1). The exponential increase of film thickness or mass with n was also observed at different Mb concentration and ionic strength in Mb adsorbate solution when pH was kept at 5.0 (Figure 3B). Hemoglobin (Hb), a larger heme protein than Mb with pI at 7.2[54] and very similar properties to Mb, also demonstrated the exponential increase of mass with n at pH 5.0 when it was assembled with oppositely charged HA into layer-by-layer films (Figure 3B). All these indicate the generality of exponential growth of $\{proteins/HA\}_n$ films under proper conditions. For protein layer-by-layer films, exponential growth was also reported previously for $\{HA/collagen\}_n$ films,[15] where collagen is a kind of protein with a rope-like fiber structure which has a shape and property similar to those of polyelectrolytes.

For $\{polycation/polyanion\}_n$ multilayer films, while linear growth with n is very common, exponential growth has also been observed for some specific systems under suitable conditions.[16−21] In particular, for some multilayer films involving HA, such as $\{CS/HA\}_n$[23] and $\{PLL/HA\}_n$ (PLL = poly(L-lysine)), [19,55] the film thickness or mass was reported to increase exponentially with n. In our present study, exponential growth of $\{CS/HA\}_n$ films was also confirmed by QCM experiments (Figure 3A). There are two interpretations for this nonlinear growth of $\{polycation/polyanion\}_n$ films. One explanation is an increase of surface roughness with deposited layers of the films, which in turn increases the surface area available for adsorption.[16,17,56] Another explanation is based on diffusion of at least one of the polyelectrolytes constituting the multilayer films in to and out of the whole films.[22,23] Theoretical modeling and calculation for weakly charged polyelectrolyte multilayer films also supports the latter interpretation.[57] For $\{Mb(pH\ 5.0)/HA\}_n$ films in our case, the first explanation does not seem reasonable since AFM experiments showed that while the surface roughness became higher for thicker films when Mb was the outermost layer, the surface became smoother with HA as the outermost layer (Figure 4). Thus, the diffusion model may be more rational to explain the exponential growth of the films.

AFM results demonstrated that when Mb was the outermost layer, more and more light spots representing the Mb aggregation "particles" were observed on the film surface with increasing bilayer numbers (Figure 4), indicating that the nonlinear increase of Mb in each bilayer with film growth happens mainly on the film surface but not inside the films. In addition, considering the relatively rigid structure of Mb and the larger size of Mb molecule ($2.5 \times 3.5 \times 4.5\ nm^3$ [32]) than that of HA, it seems difficult for Mb to physically diffuse in to and out of the whole films in adsorption, especially for the thick films. We thus speculate that the "soft" and flexible HA would be the main diffusing component and play a key role in the exponential growth of $\{Mb(pH\ 5.0)/HA\}_n$ films, although this needs to be confirmed by further experiments in future work. In the literature,[15] for $\{HA/collagen\}_n$ films, exponential growth was also attributed to diffusion of HA inside the films. According to the diffusion mechanism, when $\{Mb(pH\ 5.0)/HA\}_n$ films became thick enough, HA in adsorbate solution could not only be adsorbed on the Mb layer surface, but also be "absorbed" into the films, making the apparent adsorption amount become larger than that in the previous bilayer. On the next Mb adsorption step, in addition to the HA originally located on the film surface, which would adsorb Mb from Mb solution by electrostatic interaction, some free HA previously absorbed inside the films could also diffuse out of the films and come to the surface to combine with additional Mb from solution, making the adsorption amount of Mb become higher than that of the previous bilayer. As the films became thicker and thicker, more HA molecules may be absorbed or "entrapped" inside the films in the HA adsorption step and then diffuse out of the films in the Mb adsorption step, leading to exponential growth of the films with n.

The exponential growth of layer-by-layer films of proteins with polyelectrolytes can only be realized under appropriate conditions. First, the pH in protein adsorbate solution plays an important role, which may decide the film growth mode. For $\{Mb/HA\}_n$ films, only at pH 5.0 in Mb dipping solution, where Mb carries net positive surface charges, does film growth become exponential, whereas at pH 7.0 or 9.0, while the assembly of $\{Mb/HA\}_n$ films can be realized, the growth is linear but not exponential. Compared with the situation at pH 7.0 or 9.0, the adsorption amount of Mb and HA is much higher at pH 5.0 in each bilayer (Table 1). It seems that the high adsorption amount of proteins and polyelectrolytes in each bilayer is a necessary precondition for exponential growth of the layer-by-layer films. Second, exponential growth usually happens on the surface of thick films, so that the films have enough space to accommodate or accumulate the diffusing polyelectrolyte such as HA. Third, the growth pattern strongly depends on the type and property of polyelectrolytes used in the assembly. HA is one of the most suitable candidates. As a weak polyelectrolyte, HA has a low charge density since only one residue from the two monomer units has a carboxylic acid group that may dissociate at suitable pH (Scheme 1). HA thus shows both electrostatic and nonelectrostatic interactions (such as hydrophobic interaction and hydrogen bonding) with other assembled components, which is believed to be the key factor for exponential growth of polyelectrolyte layer-by-layer films.[16] In our previous work,[14] the assembly of $\{Mb/Dex\}_n$ layer-by-layer films was reported, where Dex represents dextran sulfate, which is also a polysaccharide. While both Dex and HA are negatively charged, Dex is a strong polyanion with much higher charge density than HA. The growth of $\{Mb/Dex\}_n$ was always linear even when Mb and Dex were oppositely charged. The theoretical calculation also suggests that the exponential growth of polyelectrolyte films with weakly charged polymers has a thermodynamic origin.[57] HA is a highly hydrated polysaccharide with good biocompatibility and can form very swelling films with proteins, which may also be helpful for the flexible HA to diffuse in to and out of the loosely structured films.

5. Conclusions

To understand the essence of interaction between proteins and polyelectrolytes in their layer-by-layer assembly and the growth mechanism of protein multilayer films, the model system of $\{Mb/HA\}_n$ films is studied systematically in the present work. For $\{Mb(pH\ 5.0)/HA\}_n$ films, the strong Coulombic interaction between oppositely charged Mb and HA makes the adsorption amount of both Mb and HA much higher than that of other $\{Mb/HA\}_n$ films built up at higher pH in Mb dipping solution. At pH 9.0, while Mb carries net negative surface charges, it can still be assembled with like-charged HA into the layer-by-layer films by localized electrostatic attraction between positive groups of Mb and negative HA or/and by reverse of pH on HA surface from higher than pI of Mb to lower than its pI. As for

$\{Mb(pH\ 7.0)/HA\}_n$ films, the hydrophobic interaction between essentially neutral Mb at pH 7.0 and HA with low charge density becomes pronounced in the assembly, especially when the ionic strength increases. The growth mode of $\{Mb/HA\}_n$ films assembled under different conditions is also different. While the buildup of $\{Mb(pH\ 7.0)/HA\}_n$ and $\{Mb(pH\ 9.0)/HA\}_n$ films linearly increases with adsorption step, growth of $\{Mb(pH\ 5.0)/HA\}_n$ films demonstrates obvious exponential character. This is most probably ascribed to the diffusion mechanism, in which some flexible HA may diffuse into the previously deposited films in the HA adsorption step and then diffuse out of the films and combine with additional Mb at the film/solution interface in the next Mb adsorption step. The nonlinear growth behavior of $\{Mb(pH\ 5.0)/HA\}_n$ films is only observed under suitable conditions, and the unique property of HA, such as low charge density, weak dissociation ability for its carboxylic acid groups, and high swelling ability, may play a key role. The profound understanding of the interaction between proteins and polyelectrolytes may guide us to find better protein layer-by-layer assembly systems, which is of importance in enzyme immobilization in a controllable way and design and construction of biodevices.

Acknowledgment. Financial support from the National Natural Science Foundation of China (20475008 and 20275006) is gratefully acknowledged.

Supporting Information Available: Four figures for CVs of $\{Mb(pH\ 5.0)/HA\}_n$ films, QCM results for assembly of $\{Cat/HA\}_n$ films, CVs of $\{Cat/HA\}_n$ films and the dependence of reduction peak currents of $\{Cat/HA\}_n$ films on the adsorption step, and RAIR spectra for pure Cat and $\{Cat/HA\}_6$/Cat films. This material is available free of charge via the Internet at http://pubs.acs.org.

References and Notes

(1) Lvov, Y. In *Protein Architecture: Interfacing Molecular Assemblies and Immobilization Biotechnology*; Lvov, Y., Mohwald, H., Eds.; Marcel Dekker: New York, 2000; pp 125−167.
(2) MacBeath, G.; Schreiber, S. L. *Science* **2000**, *289*, 1760.
(3) Decher, G. *Science* **1997**, *277*, 1232.
(4) Decher, G.; Hong, J. D. *Makromol. Chem., Marcromol. Symp.* **1991**, *46*, 321.
(5) Decher, G.; Schlenoff, J. B. In *Multilayer Thin Films: Sequential Assembly of Nanocomposite Materials*; Wiley-VCH: Weinheim, Germany, 2003.
(6) Lvov, Y. In *Nanostructured Materials, Micelles and Colloids*; Nalwa, R. W., Ed.; Handbook of Surfaces and Interfaces of Materials 3; Academic Press: San Diego, 2001; pp 170−189.
(7) Rusling, J. F. In *Protein Architecture: Interfacing Molecular Assemblies and Immobilization Biotechnology*; Lvov, Y., Mohwald, H., Eds.; Marcel Dekker: New York, 2000; pp 337−354.
(8) Lvov, Y.; Lu, Z.; Schenkman, J. B.; Zu, X.; Rusling, J. F. *J. Am. Chem. Soc.* **1998**, *120*, 4073.
(9) Ma, H.; Hu, N.; Rusling, J. F. *Langmuir* **2000**, *16*, 4969.
(10) He, P.; Hu, N.; Zhou, G. *Biomacromolecules* **2002**, *3*, 139.
(11) Ladam, G.; Gergely, C.; Senger, B.; Decher, G.; Voegel, J.-C.; Schaaf, P.; Cuisiner, F. J. G. *Biomacromolecules* **2000**, *1*, 674.
(12) Ladam, G.; Schaaf, P.; Cuisinier, F. J. G.; Decher, G.; Voegel, J.-C. *Langmuir* **2001**, *17*, 878.
(13) Schenkman, J. B.; Jansson, I.; Lvov, Y. M.; Rusling, J. F.; Boussaad, S.; Tao, N. J. *Arch. Biochem. Biophys.* **2001**, *385*, 78.
(14) He, P.; Hu, N. *J. Phys. Chem. B* **2004**, *108*, 13144.
(15) Johansson, J. A.; Halthur, T.; Herranen, M.; Soderberg, L.; Elofsson, U.; Hilborn, J. *Biomacromolecules* **2005**, *6*, 1353.
(16) Schoeler, B.; Poptoshev, E.; Caruso, F. *Macromolecules* **2003**, *36*, 5258.
(17) DeLongchamp, D. M.; Kastantin, M.; Hammond, P. T. *Chem. Mater.* **2003**, *15*, 1575.
(18) McAloney, R. A.; Sinyorr, M.; Dudnik, V.; Goh, M. C. *Langmuir* **2001**, *17*, 6655.
(19) Picart, C.; Lavalle, P.; Hubert, P.; Cuisinier, F. J. G.; Decher, G.; Schaaf, P.; Veogel, J.-C. *Langmuir* **2001**, *17*, 7414.
(20) Lavalle, P.; Picart, C.; Mutterer, J.; Gergely, C.; Reiss, H.; Voegel, J.-C.; Senger, B.; Schaaf, P. *J. Phys. Chem. B* **2004**, *108*, 635.
(21) Elbert, D. L.; Herbert, C. B.; Hubbell, J. A. *Langmuir* **1999**, *15*, 5355.
(22) Picart, C.; Mutterer, J.; Richert, L.; Luo, Y.; Prestwich, G. D.; Schaaf, P.; Voegel, J.-C.; Lavalle, P. *Proc. Natl. Acad. Sci. USA* **2002**, *99*, 12531.
(23) Richerd, L.; Lavalle, P.; Payan, E.; Zheng, X. S.; Prestwich, G. D.; Stoltz, J. F.; Schaaf, P.; Voegel, J.-C.; Picart, C. *Langmuir* **2004**, *20*, 448.
(24) Lapcik, L., Jr.; Lapcik, L.; De Smedt, S.; Demeester, J.; Chabrecek, P. *Chem. Rev.* **1998**, *98*, 2663.
(25) In *The Chemistry, Biology, and Medical Applications of Hylauronan and Its Derivatives*; Laurent, T. C., Ed.; Portland Press: London, 1998.
(26) Kujawa, P.; Moraille, P.; Sanchez, J.; Badia, A.; Winnik, F. M. *J. Am. Chem. Soc.* **2005**, *127*, 9224.
(27) Miller, M. D.; Bruening, M. L. *Langmuir* **2004**, *20*, 11545.
(28) Bellelli, A.; Antonini, G.; Brunori, M.; Springer, B. A.; Sligar, S. J. *J. Biol. Chem.* **1990**, *265*, 18898.
(29) Sauerbrey, G. *Z. Phys.* **1959**, *155*, 206.
(30) Brandrup, J.; Immergut, E. In *Polymer Handbook*; Wiley: New York, 1975; p 5.
(31) Creighton, T. E. In *Protein Structure, A Practical Approach*; IRL Press: New York, 1990; p 43.
(32) Kendrew, J.; Phillips, D.; Stone, V. *Nature* **1960**, *185*, 422.
(33) Rusling, J. F.; Nassar, A.-E. F. *J. Am. Chem. Soc.* **1993**, *115*, 11891.
(34) Bard, A. J., Faulkner, L. R. In *Electrochemical Methods*, 2nd ed. Wiley: New York, 2001.
(35) Murray, R. W. In *Electroanalytical Chemistry*; Bard, A. J. Ed.; Marcel Dekker: New York, 1984; Vol. 13, pp 191−368.
(36) Rinaudo, M.; Milas, M.; Le Dung, P. *Int. J. Biol. Macromol.* **1993**, *15*, 281.
(37) Theorell, H.; Ehrenberg, A. *Acta Chem. Scand.* **1951**, *5*, 823.
(38) Gerorge, P.; Hanania, G. *Biochem. J.* **1952**, *52*, 517.
(39) Torii, H.; Tasumi, M. In *Infrared Spectroscopy of Biomolecules*; Mantsch, H. H., Chapman, D., Eds.; John Wiley & Sons: New York, 1996; pp 1−18.
(40) Rusling, J. F.; Kumosinski, T. F. *Nonlinear Computer Modeling of Chemical and Biochemical Data*; Academic Press: New York, 1996; pp 117−134.
(41) Caruso, F.; Trau, D.; Mohwald, H.; Renneberg, R. *Langmuir* **2000**, *16*, 1485.
(42) Zhang, Z.; Chouchane, S.; Magliozzo, R. S.; Rusling, J. F. *Anal. Chem.* **2002**, *74*, 163.
(43) Lu, H.; Li, Z.; Hu, N. *Biophys. Chem.* **2003**, *104*, 623.
(44) Biesheuvel, P. M.; Cohen Start, M. A. *Langmuir* **2004**, *20*, 2785.
(45) Biesheuvel, P. M.; Wittemann, A. *J. Phys. Chem. B* **2005**, *109*, 4209.
(46) Shire, S. J.; Hanania, I. H.; Gurd, F. R. N. *Biochemistry* **1974**, *13*, 2967.
(47) Stigter, D.; Alonso, D. O. V.; Dill, K. A. *Proc. Natl. Acad. Sci. U.S.A.* **1991**, *88*, 4176.
(48) Matsui, M.; Kiyozumi, Y.; Yamamoto, T.; Mizushina, Y.; Mizukami, F.; Sakaguchi, K.; *Chem. Eur. J.* **2001**, *7*, 1555.
(49) Lu, J. R.; Su, T. J.; Howlin, B. J. *J. Phys. Chem. B* **1999**, *103*, 5903.
(50) Santos, J. H.; Matsuda, N.; Yoshida, Z. Q. T.; Takatsu, A.; Kato, K. *Surf. Interface Anal.* **2003**, *35*, 432.
(51) Lojou, E.; Bianco, P. *Langmuir* **2004**, *20*, 748.
(52) Kotov, N. A. *Nanostruct. Mater.* **1999**, *12*, 789.
(53) Alberts, B.; Bray, D.; Lewis, J.; Raff, M.; Roberts, K.; Watson, J. D. In *Molecular Biology of the Cell*, 3rd ed.; Alberts, B., Bray, D., Lewis, J., Raff, M., Roberts, K., Watson, J. D., Eds.; Garland: New York, 1994; p 89.
(54) Matthew, J. B.; Hanania, G. I. H.; Gurd, F. R. N. *Biochemistry* **1979**, *18*, 1919.
(55) Garza, J. M.; Schaaf, P.; Muller, S.; Ball, V.; Stoltz, J. F.; Voegel, J.-C.; Lavalle, P. *Langmuir* **2004**, *20*, 7298.
(56) Kolarik, L.; Furlong, D. N.; Joy, H.; Struijk, C.; Rowe, R. *Langmuir* **1999**, *15*, 8265.
(57) Biesheuvel, P. M.; Cohen Stuart, M. A. *Langmuir* **2004**, *20*, 4764.